ACS OMEGA

Article

Cite This: ACS Omega 2018, 3, 13576−13583

http://pubs.acs.org/journal/acsodf

In Vitro Selection and Characterization of a Single-Stranded DNA Aptamer Against the Herbicide Atrazine

Kevin M. Abraham,[†,‡] Mina Roueinfar,[†,‡] Alex T. Ponce,[†] Mia E. Lussier,[†] Danica B. Benson,[†] and Ka Lok Hong*[,†]

[†]Department of Pharmaceutical Sciences, Nesbitt School of Pharmacy, and [‡]Department of Biology, College of Science and Engineering, Wilkes University, 84 W. South Street, Wilkes-Barre, Pennsylvania 18766, United States

Supporting Information

ABSTRACT: Atrazine is an herbicide that is widely used in crop production at about 70 million pounds per year in the United States. Its widespread use has led to contamination of groundwater and other aquatic systems. It has resulted in many serious environmental and human health issues. This study focuses on the identification and characterization of a single-stranded DNA (ssDNA) aptamer that binds to atrazine. In this study, a variation of the systematic evolution of ligands by exponential enrichment (SELEX) process was used to identify an aptamer, which binds to atrazine with high affinity and specificity. This SELEX focused on inducing the aptamer's ability to change conformation upon binding to atrazine, and stringent negative target selections. After 12 rounds of in vitro selection, the ssDNA aptamer candidate R12.45 was chosen and truncated to obtain a 46-base sequence. The binding affinity, specificity, and structural characteristics of this truncated candidate was investigated by using isothermal titration calorimetry, circular dichroism (CD) analysis, SYBR Green I (SG) fluorescence displacement assays, and gold nanoparticles (AuNPs) colorimetric assays. The truncated R12.45 candidate aptamer bound to atrazine with high affinity (K_d = 3.7 nM) and displayed low cross-binding activities on structurally related herbicides. In addition, CD analysis data indicated a target induced structural stabilization. Finally, SG assays and AuNPs assays showed nonconventional binding activities between the truncated R12.45 aptamer candidate and atrazine, which warrants future studies.

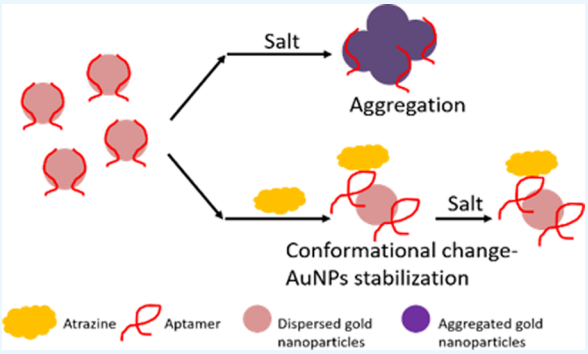

INTRODUCTION

Atrazine is an herbicide that is widely used in crop production. It is used to prevent the growth of broad-leafed weeds in both agricultural and residential environments. Although the European Union has banned atrazine since 2003, it is the second most widely used herbicide in the United States with an average of over 70 million pounds of atrazine being used per year.[1] Atrazine's widespread use and persistence has led to the contamination of groundwater and other aquatic systems.[2] This contamination disrupts hormones in animals and is linked to cancers and birth defects.[2,3] Studies demonstrated that atrazine inhibits the production of testosterone and induces the production of estrogen, thus chemically-castrating many types of animals. Amphibians and fish are at the greatest risk because of living in an aquatic system.[3,4] This type of endocrine disruption from atrazine has the potential to affect humans and other mammals.[3] The wide spectrum of atrazine's described detrimental effects has led to the investigation of low-cost, reversible novel binding elements specific to atrazine for rapid biosensing applications.[5−7]

Aptamers are nucleic acid-based molecular recognition elements that were first described independently by the Gold group and the Szostak group.[8,9] These functional single-stranded nucleic acids can fold into 3-dimensional conformations, and bind to user-defined target molecules with very high affinity and specificity. Aptamers are identified through an iterative in vitro selection process, termed, systematic evolution of ligands by exponential enrichment (SELEX). This process involves repeated incubation of a large random oligonucleotide library ($\sim 10^{15}$) with the user defined target, partitioning between the target-bound and nonbound library molecules, and amplification.[10] Previously, there were two single-stranded DNA (ssDNA) aptamers identified to target atrazine.[6,7] Sanchez described using capillary electrophoresis-based SELEX (CE-SELEX) to identify a ssDNA aptamer specific for atrazine with a dissociation constant (K_d) of 890 nM.[6] Williams et al. also identified a ssDNA aptamer that binds to atrazine using a variation of the SELEX process heavily emphasized on directing the library molecules away from binding to nondesired targets or negative targets.[7] The selected aptamer had a K_d reported in the subnanomolar range and high specificity toward atrazine.

Received: August 1, 2018
Accepted: October 8, 2018
Published: October 19, 2018

DOI: 10.1021/acsomega.8b01859
ACS Omega 2018, 3, 13576−13583

ssDNA aptamers have been extensively investigated in biosensing applications because of their low-cost and reversible denaturation.[11,12] Aptamers with conformational changes upon target binding and recognition have even higher value in biosensor integration.[10] Different SELEX variants have been developed to intentionally identify aptamers with target-induced conformational change properties, such as GO-SELEX and Capture-SELEX.[13,14] Although both previously reported atrazine binding aptamers were identified with respectable affinity and specificity, it is unknown if there is a target-induced conformational change present in either reported full length aptamers. The aim of this study was to adopt a previously described Capture-SELEX protocol in order to identify a ssDNA aptamer specific for atrazine that would have a target-induced conformational change.[15,16] The ssDNA oligonucleotide library utilized in this study has been successfully screened for multiple aptamers bound to small molecules and protein targets.[7,17−22]

At the conclusion of this study, a truncated ssDNA aptamer with high affinity and specificity for atrazine was identified using a modified Capture-SELEX protocol in combination with a stringent negative selection scheme (Decoy-SELEX). Structural studies revealed target-induced conformational stabilization that was not demonstrated in previously reported atrazine binding aptamers. In addition, this study demonstrated the generalization of the Capture-SELEX protocols to a ssDNA oligonucleotide library that was not specifically designed for the Capture-SELEX protocol.

RESULTS AND DISCUSSION

Twelve rounds of SELEX were performed to identify a ssDNA aptamer which targets atrazine (Table 1). Detailed protocols can be found in the Experimental Section. In brief, the random ssDNA oligonucleotide library was captured on cDNA probe-coated magnetic beads. Atrazine was introduced to the system to induce the release of library molecules from the cDNA probe. The solution containing atrazine-bound library molecules was partitioned by magnets, and subsequently amplified by polymerase chain reaction (PCR). ssDNA molecules were retrieved before being subjected to another round of in vitro selection (Figure 1). Twenty five, thirty two, thirty, and forty six of post round 3, 6, 9, and 12 library clones were sequenced and analyzed for consensus sequence family, respectively. Sequences obtained from post round 12 selection were analyzed by Mfold for secondary structures and Gibbs free energy values (ΔG).[23] One candidate sequence, designated R12.45 was highly conserved in multiple sequence families after alignment analysis (Figure 2). Mfold predicted that the secondary structure of the 5′ constant region of R12.45 to be partially hybridizing with the random region of the sequence. The first 10 bases of the oligonucleotide library were captured on probe cDNA before atrazine was introduced

Table 1. SELEXs Scheme for Atrazine Binding Aptamer Identification

rounds	negative selection	time (min)	positive selection	time (min)	cDNA length
1			atrazine 50 μM	30	8
2			atrazine 25 μM	30	8
3			atrazine 15 μM	30	8
4	simazine 0.5 μM	10	atrazine 15 μM	30	8
5	simazine 1 μM	15	atrazine 10 μM	30	8
6	propazine 0.5 μM	15	atrazine 5 μM	15	8
7	propazine 1 μM	20	atrazine 2.5 μM	10	9
8	cyanazine 0.5 μM	20	atrazine 1 μM	5	9
9	cyanazine 1 μM	25	atrazine 0.5 μM	2.5	9
10	terbuthylazine 0.5 μM	25	atrazine 0.1 μM	2	10
11	terbuthylazine 0.5 μM	30	atrazine 50 nM	1.5	10
12	simazine 1 μM, propazine 1 μM, cyanazine 1 μM, terbuthylazine 1 μM, 30 min each	120	atrazine 10 nM	1	10

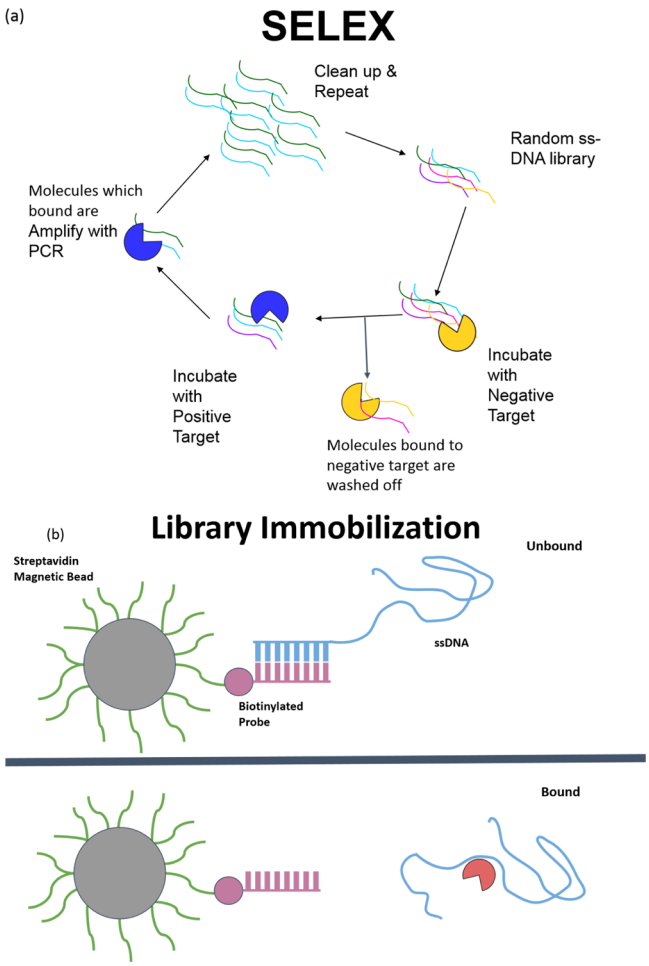

Figure 1. (a) Illustration of the systematic evolution of ligand by exponential enrichment process. Library molecules that bind to negative targets (undesired targets) are washed away, and those that bind to the positive target (atrazine in this study) are retrieved and amplified by PCR. This completes one round of SELEX. (b) Illustration of the library immobilization process for the modified Capture-SELEX. Biotinylated cDNA probes are first captured on streptavidin coated magnetic beads. Library ssDNA molecules dehybridized by positive target induction are retrieved and subsequently amplified.

DOI: 10.1021/acsomega.8b01859
ACS Omega 2018, 3, 13576−13583

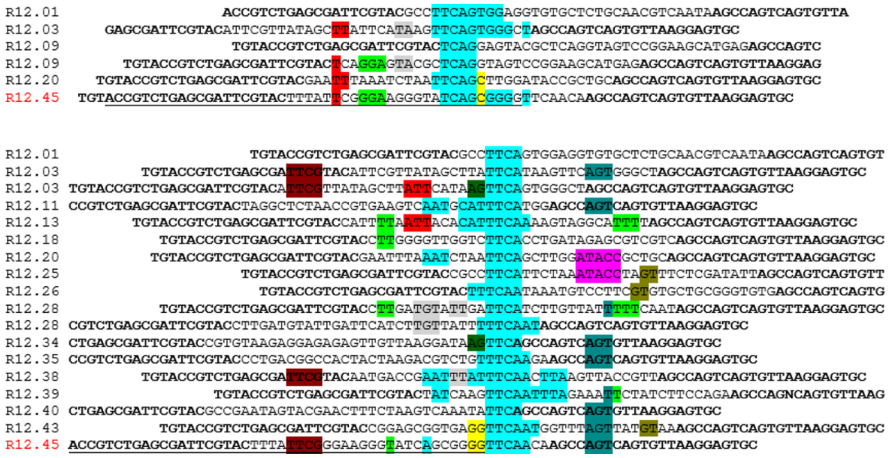

Figure 2. Representative families of sequences obtained from postround 12 sequencing. Bold letters are partial constant regions. R12.45 candidate sequences shared consensus sequences with other clones. The center for alignment in each family is highlighted in turquoise color. The underlined portion of R12.45 was truncated out for characterization.

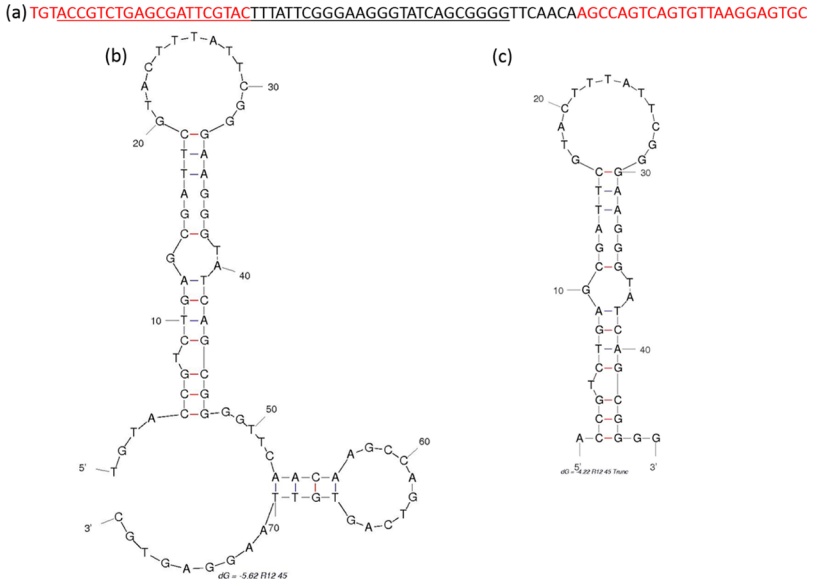

Figure 3. (a) Full sequence of the R12.45 candidate aptamer. Red color represents the constant regions and the underlined region represents the truncated region. (b) Secondary structure of the full R12.45 candidate aptamer predicted by Mfold.[23] (c) Secondary structure of the R12.45 truncated candidate aptamer predicted by Mfold.[23] Images are from free domain and are specific for the given sequences and binding condition.

in the system, which suggests the target induced dehybridization of the single-stranded oligonucleotide from the cDNA (Figure 3a). The predicted secondary structure contained one long hairpin structure comprised with partial 5′ constant region and approximately 74% of the random region, and a small second hairpin comprised with 12% of the random region and partial 3′ constant region (ΔG = −5.62 kcal/mol). It has been reported that the constant region can also participate in binding events, and therefore may be included in candidate aptamer sequence analysis.[24−28] Because of the cost and efficiency of oligonucleotide chemical synthesis, R12.45 candidate sequence was truncated into a 46-base long hairpin structure for binding and structural characterization (ΔG = −4.22 kcal/mol) (Figure 3b).

The binding affinity between the truncated R12.45 (R12.45 Trunc.) and atrazine was measured by automatic isothermal titration calorimetry (ITC, MicroCal Auto-iTC200 by GE). Three independent assays were performed to optimize the binding conditions. Two hundred microliter of 50 μM atrazine was titrated into four hundred microliter of 10 μM 12.45 Trunc. candidate aptamer in the sample cell at 25 °C, and the equilibrium dissociation constant (K_d) was estimated to be 3.7 nM based on nonlinear regression model analysis by companion software, where n-value was fitted as a variable (Figure 4, Table S1). The quality of data obtained from ITC experiments can be described by the Wiseman coefficient $c = n \times [\text{aptamer}]/K_d$, where n represents the number of binding site. It was reported that c values range from 1 to 1000 were needed to reflect reliable ITC data.[29] It is to be noted that an n-value of less than 1 suggests multiple binding positions may be present on the ligand.[30] The reported ITC data had a calculated c value of 162, where the molar ratio between macromolecule (aptamer) and ligand (atrazine) was 1:5. In contrast to another experiment performed with a molar ratio of 1:10, where the c value was less than 1 (3.9×10^{-5}), the current data and the experimental setup suggested its validity. At the given atrazine concentration (50 μM), the binding between the aptamer candidate and the ligand was complete. It

DOI: 10.1021/acsomega.8b01859
ACS Omega 2018, 3, 13576−13583

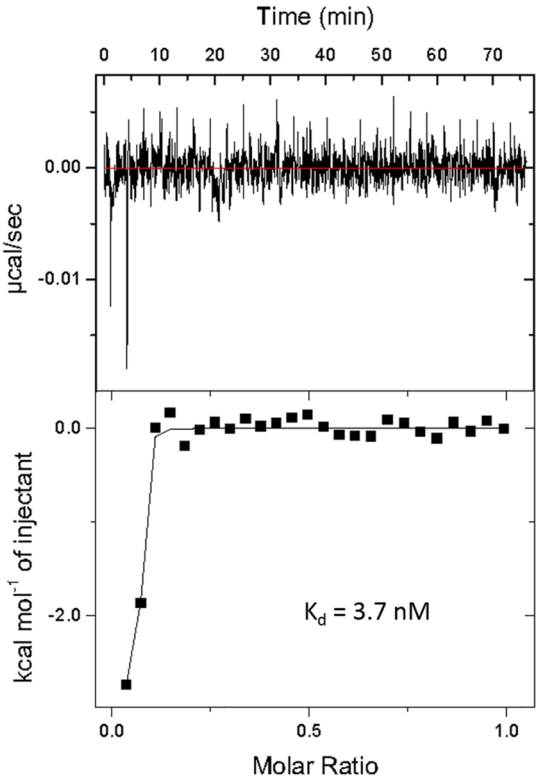

Figure 4. ITC analysis of binding affinity between R12.45 Trunc. candidate aptamer and its target, atrazine.

is important to be noted that while the concentration of the ligand may be increased to enhance the heat response, the molar ratio must be maintained. However, it has been reported that increased aptamer concentration may lead to increased K_d resulting from interaptamer interaction.[31] Therefore, the concentration of both the aptamer and atrazine utilized were optimal for this experiment.

The K_d value determined in this study was consistent with other published small molecule binding ssDNA aptamers.[32−34] The selection stringency or pressure was increased by (1) lengthening the cDNA probe bases, thus, increasing the difficulty for breaking the hybridization force, (2) decreasing the incubation time and concentrations of atrazine, thus, only the library molecules that bind to atrazine in a quick and strong fashion would be retrieved. This adopted selection strategy validated previously published selection schemes (Decoy-SELEX).[19,20]

The specificity of the R12.45 Trunc. was characterized by using SYBR Green I (SG) fluorescence displacement assay as previously described.[35] SG is a green fluorescence dye specific for double-stranded DNA by means of DNA intercalation. The dye itself does not have a fluorescence signal and is commonly used in reverse transcription PCR (RT-PCR) for template amplification monitoring. The assay principle was based upon the binding of target molecules to the aptamer, and the displacement of intercalated SG dyes from partially hybridized regions, thus decreasing the fluorescence signal. However, multiple assays result showed the binding of atrazine to R12.45 Trunc. candidate aptamer produced higher fluorescence signal in the presence of SG when compared to control samples without atrazine. The cross-binding activity of R12.45 Trunc. on negative targets used in the selection were assayed with the same experimental set up (Table 2). Interestingly, the

Table 2. Cross-Reactivity Data of R12.45 Trunc. Aptamer Candidate[a]

target	normalized average fluorescence	standard deviation	*p*-value	selectivity ratio
atrazine	0.0716	0.0074		
simazine	0.0389	0.0095	0.031	1.84
propazine	0.0218	0.022	0.047	3.23
terbuthylazine	0.0213	0.023	0.048	3.32
cyanazine	−0.02178	0.035	0.033	Neg.[b]

[a]For each negative target (1 μM), 1 × standard deviation is presented with normalized average fluorescence. Each set of experiments was performed in duplicate. A one-tailed student's *t*-test was performed between atrazine and negative targets to determine the statistical significance ($p < 0.05$). The selectivity ratio represents binding to atrazine is higher than the negative targets. [b]Neg. denotes minimal binding of R12.45 Trunc. to cyanazine, and therefore a very large selectivity ratio.

normalized average fluorescence signal of all negative targets binding to R12.45 Trunc. was lower than the signal recovered from binding to atrazine. This result was contradictory to the assay principle described in the literature.[35,36] In order to investigate this phenomenon further, varying concentration of atrazine (1 nM to 1 μM) were tested in a SG standard assay. A trend of increasing fluorescence signal at low concentrations of atrazine followed by a decrease in the fluorescence signal at high concentrations of atrazine was observed in multiple repeated assays (Figure S1). The same experimental setup was also subjected to a melting experiment with the use of a real-time PCR system (StepOnePlus by Thermo Scientific). Normalized fluorescence signals at low concentrations of atrazine were higher than signals of the buffer control (Figure S2). This trend continued as the temperature increased. The trend of the fluorescence signals of atrazine led to our hypothesis that the binding of atrazine at low concentration initially stabilizes the secondary structures of R12.45 Trunc., thus, leading to increased amount of SG intercalation, and higher levels of the fluorescence signal. In addition, it suggested that SG was starting to be displaced when atrazine was in excess. It is to be noted that the fluorescence signal recovered from cyanazine addition was lower than the buffer control, which suggested the nonspecific interaction between R12.45 Trunc. and cyanazine was different than the interaction with other negative targets. This was likely due to the presence of a cyano functional group, and a relatively larger degree of structural differences when compared to other triazine herbicides (Figure S3).

Circular dichroism (CD) analysis was performed to further study the secondary structure in R12.45 Trunc. candidate aptamer upon atrazine binding (Figure 5). The CD spectra showed a characteristic negative band at around 245 nm, and a positive band at around 270 nm. This confirmed R12.45 Trunc. assumed a B-form DNA structure.[37] The CD amplitude of R12.45 Trunc. was reduced upon the addition of atrazine. Although the global conformation of the aptamer did not change, the reduction in amplitude indicated a transition of a B-form duplex, to a hairpin.[38] Previous study reported hairpin, bulges and stem-loop structures in aptamers are responsible for target binding.[39] As mentioned previously, the ΔG value of R12.45 Trunc. was −4.22 kcal/mol, which indicates a relatively less stable structure when compared to the full length R12.45. The CD spectra changes suggested the binding of atrazine stabilized the overall secondary structure via the hairpin

DOI: 10.1021/acsomega.8b01859
ACS Omega 2018, 3, 13576−13583

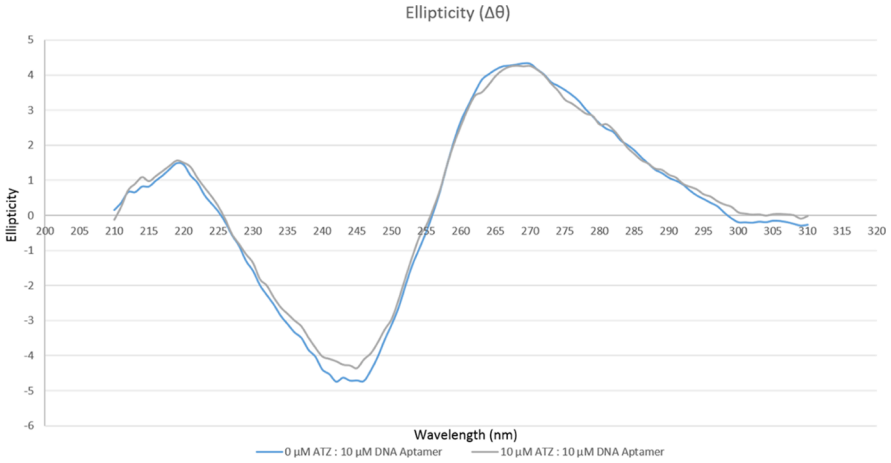

Figure 5. CD analysis of R12.45 Trunc. candidate aptamer in the present or absent of atrazine (ATZ: atrazine).

position, while maintaining the global B-form DNA conformation.

Gold nanoparticle (AuNP) colorimetric assay has been commonly utilized as a rapid detection platform for aptamer–target binding.[36,40] In brief, the assay principle relies on the pink-red to blue-purple shift in localized surface plasmon resonance observed in AuNPs aggregation. Multiple studies showed ssDNA aptamers coated AuNPs resisted salt induced aggregation, the blue-purple color shift was not observed. Upon the addition of the target, ssDNA aptamer detached from AuNPs, the salt induced blue-purple color shift was observed. This change in color could be quantified with absorbance measurement at 520 and 650 nm. A previously reported AuNPs colorimetric assay protocol was adopted to further investigate the binding characteristics between R12.45 Trunc. and atrazine.[36] Cyanazine was chosen as the negative control based on the result obtained from the SG fluorescence displacement assay. Unexpectedly, there was no salt induced AuNPs aggregation observed when different concentrations (as high as 100 μM) of atrazine were added to the aptamer coated AuNPs (Figure 6). On the other hand, a statistically significant aggregation was observed when 100 μM of cyanazine was added to the same system. This observation was again contradicted with the majority of literature.[36,40,41] However, two previous studies showed similar AuNPs aggregation patterns observed in this current study.[42,43] Chavez et al.

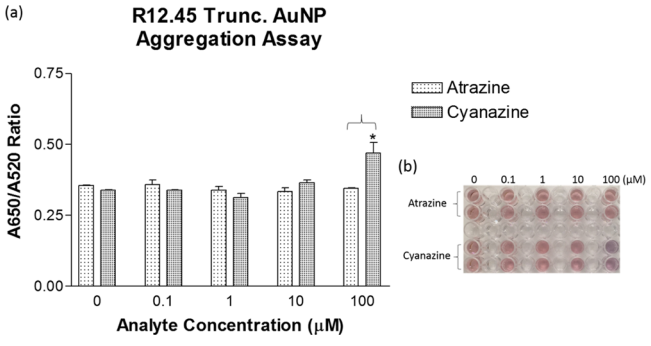

Figure 6. (a) Aggregation response to atrazine and cyanazine addition quantified by absorbance ratio. *One-tailed student's *t*-test was performed between atrazine and cyanazine to determine the statistical significance ($p < 0.05$). (b) Digital image of the samples represented in (a).

reported an AuNPs colorimetric detection assay utilizing the riboflavin binding aptamer (RBA).[43] The study showed the addition of riboflavin to RBA coated AuNPs increased RBA stability on AuNPs surfaces. When salt was added to the system, no aggregation was observed. On the other hand, when a nontarget small molecule, 2-quinoxaline carboxylic acid was added to the system, a blue-purple color shift was observed after salt addition. Smith et al. additionally investigated AuNPs colorimetric detection assay utilizing two different cocaine binding aptamers, MN4 and MN6.[42] MN4 was a known aptamer for cocaine with no conformational change upon target recognition. MN6 on the other hand, displayed a conformational change upon cocaine binding. It was reported that MN6 coated AuNPs remained in the nonaggregated state upon cocaine and salt addition. This was because of target-induced structural stabilization. The AuNPs colorimetric assay in this study demonstrated a result similar to the previous two studies. This also supports our hypothesis generated during our SG fluorescence displacement assay, in that, binding of atrazine to R12.45 Trunc. stabilizes the secondary structure of the aptamer, and thus supported the contradictory result from the fluorescence displacement assay.

There are two previously reported atrazine binding aptamers.[6,7] At-Apt-25 aptamer, identified by Sanchez did not have statistically significant selectivity between atrazine and simazine, a trizaine herbicide which differs only by one methyl group.[6] R12.45 Trunc. displayed similar selectivity between atrazine and simazine when compared to the aptamer (R12.23) identified by Williams et al. study.[7] Upon comparing previously published atrazine binding aptamer sequences (Figure S4), there are higher similarities between the truncated R12.23 and R12.45 Trunc. after alignment near the center of R12.45 Trunc than between At-Apt-25. This suggests high affinity atrazine binding to ssDNA aptamer may be conserved within a few nucleotides. Notably, that this study utilized the same ssDNA oligonucleotide library design (RMWN34) as Williams et al. This library was first designed for general SELEX methodology. The current study showed the success of adopting a Capture-SELEX protocol to an existent library without any sequence modifications. This has validated the robustness of the Capture-SELEX protocol previously described and that it may be generalized to other oligonucleotide libraries.[15,16] Williams et al. utilized target immobilized magnetic bead based in vitro selection, which did not have specific selection conditions for screening aptamers with target induced

DOI: 10.1021/acsomega.8b01859
ACS Omega 2018, 3, 13576–13583

conformational change or structural stabilization. It is generally agreed in the aptamer research field that it is particularly more challenging to identify aptamers specific for small molecules than for proteins.[44,45] This is largely because of the less binding motifs on small molecules. It is interesting to see the different SELEX strategies can be utilized on the same oligonucleotide library, and ultimately identify two different aptamers that bind to the same small molecule target.

CONCLUSIONS

This study identified a new ssDNA aptamer that binds to atrazine with high affinity and specificity. These are attractive features for future biosensor development. It also revealed nonconventional binding characteristics of R12.45 Trunc. aptamer. This phenomenon warrants further studies involving characterization comparison between the R12.23 and R12.45 Trunc. It is known that the predicted stability of the R12.23 is higher than that of R12.45 Trunc. One pervious study showed the truncated R12.23 aptamer (34-mer) did not assume conformational change upon atrazine binding.[46] The potential different binding characteristics are currently under investigation by our group.

EXPERIMENTAL SECTION

In Vitro Selection for Atrazine-Specific ssDNA Aptamer. In brief, the ssDNA oligonucleotide library utilized in this study was previously designed by the Sooter Laboratory at WVU, and termed RMWN34.[7] The DNA library was commercially synthesized by TriLink Biotechnologies with PAGE purification. NanoLink streptavidin magnetic bead was also purchased from TriLink Biotechnologies. The primer sequences were purchased from Eurofins Genomics with desalt purification. The cDNA capture probes were purchased from IDT with desalt purification. Sequences are shown below.

Library: 5′-TGTACCGTCTGAGCGATTCGTAC-N_{34}-AGCCAGTCAGTGTTAAGGAGTGC-3′

Forward primer: 5′-TGTACCGTCTGAGCGATTCGTAC-3′

Reverse primer: 5′-GCACTCCTTAACACTGACTGGCT-3′

Biotinylated reverse primer: 5′-biotin-GCACTCCTTAACACTGACTGGCT-3′

8-mer cDNA capture probe: 5′-ACGGTACA-biotin-3′

9-mer cDNA capture probe: 5′-GACGGTACA-biotin TEG-3′

10-mer cDNA capture probe: 5′-AGACGGTACA-biotin TEG-3′

Atrazine, simazine, propazine, terbuthylazine, and cyanazine were all purchased from Sigma with analytical standards.

The selection process was adopted from previously described protocols.[15,16] In brief, 60 μL of streptavidin coated magnetic beads suspended in selection buffer (100 mM NaCl, 20 mM Tris-HCl, and 5 mM $MgCl_2$, pH 7.4) were incubated with 3.6 μL of 1 M biotinylated cDNA probe for 30 min at room temperature. After the incubation, the bead suspension was washed with the selection buffer for three times to the remove nonspecifically adhered cDNA probe. Approximately 10^{15} copies of ssDNA from the library dissolved in selection buffer was first denatured at 95 °C for 5 min, then snapped cool to 4 °C, and, finally, equilibrated to room temperature. The library was serially added to 20 μL of cDNA coated magnetic beads for a total of 3 times. The final prepared library captured magnetic beads were washed in selection buffer for 3 times to remove nonspecifically adhered library molecules. UV measurement (NanoDrop ND-2000c spectrophotometer, Thermo Scientific) was utilized to monitor the library capturing efficiency. The library preparation was performed immediately before each round of selection. The melting temperatures between all cDNA probes and the library in the presence of 5 mM Mg^{2+} (selection buffer condition) were first estimated with free software (Promega). It was estimated that probe lengths from eight to ten were suitable for aneling and dehybridizing at around room temperatures. The cDNA probe length increased as the selection progress to raise selection pressure (Table 1).

During rounds 1−3, incubation of the library with only atrazine was performed for a predetermined amount of time (Table 1). The target bound, and unbound sequences were partitioned using the magnet. The bound portion of the library was retained. Starting from round 4 on, negative targets were introduced before atrazine incubation (Table 1). The negative target bound portion of the library was extracted and discarded, and the remaining library was incubated with atrazine. Once the incubation with atrazine was completed, the bound sequences were retrieved for the next step. All herbicides used in the study were dissolved in 10% methanol-selection buffer due to low water solubility. All selection steps were performed at room temperature. The multiple negative targets selection scheme was adopted from previously described Decoy-SELEX.[19,20]

After each round of the selection, the solution containing the atrazine bound library molecules was first dialyzed with a 2k MWCO dialysis device (Thermo Scientific) to remove excess atrazine in the solution. The remaining solution containing the atrazine bound ssDNA molecules were subjected to PCR. The PCR mixture conditions and thermal cycling conditions were prepared identically as previously described.[7] The PCR product was purified with IBI purification kit (IBI Scientific) according to manufacturer's protocol. At least 10^{13} copies of amplified dsDNA were obtained with large scale PCR (4−5 mL). Purified dsDNA was subjected to single strand separation and ethanol precipitation to retrieve the forward strand DNA exactly as previously described.[7]

Cloning and Sequencing of the Atrazine-Binding ssDNA Aptamer. In brief, the ssDNA oligonucleotide library of post rounds 3, 6, 9, and 12 were cloned into TOP10 competent cells (Thermo Scientific), and plasmid DNA was extracted as previously described. The plasmid DNA was sequenced by Eurofins Genomics. The truncated candidate aptamer sequence, R12.45 Trunc. was commercially synthesized by Eurofins Genomics with PAGE purification.

SG Fluorescence Displacement Assay. In brief, the assay was performed as previously described with slight modifications.[35] R12.45 Trunc. at 10 μM was prepared in 10% methanol selection buffer (10% v/v methanol, 100 mM NaCl, 20 mM Tris-HCl, and 5 mM $MgCl_2$, pH 7.4). It was then denatured at 95 °C for 5 min, then snapped cool to 4 °C, and finally equilibrated to room temperature. Four microliter of 1 × SG was mixed with 10 μM of aptamer solution at 1 to 1 ratio. Atrazine concentration was prepared from 1 nM to 1 μM in the same selection buffer. Atrazine and SG-aptamer mixture were mixed to have a final volume of 125 μL. Samples were prepared in duplicate. Negative controls were atrazine alone and atrazine with SG and buffer with SG-aptamer. All samples were placed in a black 96-well microplate and fluorescence

DOI: 10.1021/acsomega.8b01859
ACS Omega 2018, 3, 13576−13583

signal was measured in a FLx800 microplate reader (Biotek) with excitation at 490 nm and emission at 520 nm. All fluorescence readings were normalized with $((F - F_0)/F_0)$, where F_0 was the fluorescence reading from the buffer control. Three independent assays were performed as described. The same experimental setup was also utilized in RT-PCR melting experiment.

To determine the specificity of R12.45 Trunc. A similar experiment was performed, where all herbicides used in the selection were prepared at 1 μM. Samples were prepared in duplicates with three independent assays performed. Representative results were presented. Data was averaged and the standard deviation was calculated. The statistical significant difference of the means ($p < 0.05$) was determined with the one-tailed student *t*-test.

CD Studies. A JASCO J-1500 CD spectrophotometer (JASCO) was used to study the binding characteristic between R12.45 Trunc. and atrazine. The 10% methanol selection buffer was first scanned for three times with a wavelength range from 210 to 310 nm at 50 nm/min scanning speed, in a 1 mm path length quartz cuvette. The spectra was averaged and subtracted from the actual sample scans. The solution of 10 μM R12.45 Trunc. in the identical buffer was scanned with the exact same parameter, and served as reference. Lastly, the solution of 10 μM aptamer and 10 μM atrazine were also scanned to compare. All spectral data was averaged and analyzed with the spectra manager software from the manufacturer.

AuNPs Colorimetric Assay. The AuNPs were purchased from Nano Composix. Manufacturer specification sheet indicated an average particle diameter of 9.8 ± 0.8 nm at 9.5 nM particle concentration. The assay was performed as previously described. In brief, 6 μL of R12.45 Trunc. at 10 μM in 10% methanol water and 135 μL of AuNPs from the stock were incubated for 30 min at room temperature. Targets (atrazine and cyanazine) at varying concentrations (100 nM to 100 μM, 10% methanol water) in 243 μL total volume were added to the aptamer−gold mixture and incubated for 30 min at room temperature. Lastly, 6 μL of 1 M sodium chloride solution was added to each mixture for 5 min. The aggregation pattern was observed by naked eye, and in addition transferred to a clear 96-well plate for digital imaging, and absorbance scan at 520 and 650 nm with a μQuant plate reader (Biotek). Samples were prepared in duplicate. Three successful independent assays were performed. Representative data was averaged and standard deviation was calculated. Statistical significant difference of the means ($p < 0.05$) was determined with the one-tailed student *t*-test.

■ ASSOCIATED CONTENT

Supporting Information

The Supporting Information is available free of charge on the ACS Publications website at DOI: 10.1021/acsomega.8b01859.

Binding thermodynamic values of ITC experiments; representative data from SYBR Green standard assay; SYBR Green standard melting experiment; chemical structures of all the herbicides used in the selection scheme; sequence comparison of different atrazine binding aptamers (PDF)

■ AUTHOR INFORMATION

Corresponding Author

*E-mail: kalok.hong@wilkes.edu. Phone: +1-570-408-4296. Fax: +1-570-408-4299.

ORCID

Ka Lok Hong: 0000-0002-8299-7128

Notes

The authors declare no competing financial interest.

■ ACKNOWLEDGMENTS

This work was supported by Wilkes University Faculty Development Type I Grant, Wilkes University Research and Scholarship Funds. K.M.A., and M.R. were supported in part by Wilkes University Summer Mentoring Grant. The authors would like to acknowledge Dr. Neela Yennawar and Julia Fecko from the Penn State Automated Biological Calorimetry Facility—University Park, PA for their assistance with the ITC and NSF-MRI award DBI-0922974 (Bevilacqua et al. 2009).

■ REFERENCES

(1) Brassard, M. G. L.; Stavola, A.; Lin, J.; Turner, L. *Atrazine: Analysis of Risks*; USEP Agency, 2003.

(2) Rossmeisl, C. M.; Hetrick, J. A.; et al. *Refined Ecological Risk Assessment for Atrazine*; U.S. Environmental Protection Agency, 2016.

(3) Fan, W.; Yanase, T.; Morinaga, H.; Gondo, S.; Okabe, T.; Nomura, M.; Komatsu, T.; Morohashi, K.-I.; Hayes, T. B.; Takayanagi, R.; Nawata, H. Atrazine-Induced Aromatase Expression Is SF-1 Dependent: Implications for Endocrine Disruption in Wildlife and Reproductive Cancers in Humans. *Environ. Health Perspect.* **2007**, *115*, 720−727.

(4) Suzawa, M.; Ingraham, H. A. The Herbicide Atrazine Activates Endocrine Gene Networks via Non-Steroidal NR5A Nuclear Receptors in Fish and Mammalian Cells. *PLoS One* **2008**, *3*, No. e2117.

(5) Madianos, L.; Tsekenis, G.; Skotadis, E.; Patsiouras, L.; Tsoukalas, D. A highly sensitive impedimetric aptasensor for the selective detection of acetamiprid and atrazine based on microwires formed by platinum nanoparticles. *Biosens. Bioelectron.* **2018**, *101*, 268−274.

(6) Sanchez, P. E. DNA Aptamer Development for Detection of Trazine and Protective Antigen Toxin using Fluorescence Polarization. Ph.D. Theses, University of California, Riverside, 2012.

(7) Williams, R.; Crihfield, C.; Gattu, S.; Holland, L.; Sooter, L. In Vitro Selection of a Single-Stranded DNA Molecular Recognition Element against Atrazine. *Int. J. Mol. Sci.* **2014**, *15*, 14332−14347.

(8) Tuerk, C.; Gold, L. Systematic evolution of ligands by exponential enrichment: RNA ligands to bacteriophage T4 DNA polymerase. *Science* **1990**, *249*, 505−510.

(9) Ellington, A. D.; Szostak, J. W. In vitro selection of RNA molecules that bind specific ligands. *Nature* **1990**, *346*, 818−822.

(10) Hong, K. L.; Sooter, L. J. Single-Stranded DNA Aptamers against Pathogens and Toxins: Identification and Biosensing Applications. *BioMed Res. Int.* **2015**, *2015*, 419318.

(11) Mishra, G.; Sharma, V.; Mishra, R. Electrochemical Aptasensors for Food and Environmental Safeguarding: A Review. *Biosensors* **2018**, *8*, 28.

(12) Zhang, W.; Liu, Q.; Guo, Z.; Lin, J. Practical Application of Aptamer-Based Biosensors in Detection of Low Molecular Weight Pollutants in Water Sources. *Molecules* **2018**, *23*, 344.

(13) Park, J.-W.; Tatavarty, R.; Kim, D. W.; Jung, H.-T.; Gu, M. B. Immobilization-free screening of aptamers assisted by graphene oxide. *Chem. Commun.* **2012**, *48*, 2071−2073.

(14) Nutiu, R.; Li, Y. In vitro selection of structure-switching signaling aptamers. *Angew. Chem., Int. Ed.* **2005**, *44*, 1061−1065.

(15) Martin, J. A.; Chávez, J. L.; Chushak, Y.; Chapleau, R. R.; Hagen, J.; Kelley-Loughnane, N. Tunable stringency aptamer

DOI: 10.1021/acsomega.8b01859
ACS Omega 2018, 3, 13576−13583

selection and gold nanoparticle assay for detection of cortisol. *Anal. Bioanal. Chem.* **2014**, *406*, 4637−4647.
(16) Martin, J. A.; Smith, J. E.; Warren, M.; Chávez, J. L.; Hagen, J. A.; Kelley-Loughnane, N. A method for selecting structure-switching aptamers applied to a colorimetric gold nanoparticle assay. *J. Visualized Exp.* **2015**, No. e52545.
(17) Hong, K.; Battistella, L.; Salva, A.; Williams, R.; Sooter, L. In vitro selection of single-stranded DNA molecular recognition elements against S. aureus alpha toxin and sensitive detection in human serum. *Int. J. Mol. Sci.* **2015**, *16*, 2794−2809.
(18) Hong, K. L.; Maher, E.; Williams, R. M.; Sooter, L. J. In Vitro Selection of a Single-Stranded DNA Molecular Recognition Element against Clostridium difficile Toxin B and Sensitive Detection in Human Fecal Matter. *J. Nucleic Acids* **2015**, *2015*, 808495.
(19) Hong, K.; Sooter, L. In Vitro Selection of a Single-Stranded DNA Molecular Recognition Element against the Pesticide Fipronil and Sensitive Detection in River Water. *Int. J. Mol. Sci.* **2017**, *19*, 85.
(20) Hong, K. L.; Yancey, K.; Battistella, L.; Williams, R. M.; Hickey, K. M.; Bostick, C. D.; Gannett, P. M.; Sooter, L. J. Selection of Single-Stranded DNA Molecular Recognition Elements against Exotoxin A Using a Novel Decoy-SELEX Method and Sensitive Detection of Exotoxin A in Human Serum. *BioMed Res. Int.* **2015**, *2015*, 417641.
(21) Williams, R.; Maher, E.; Sooter, L. In vitro selection of a single-stranded DNA molecular recognition element for the pesticide malathion. *Comb. Chem. High Throughput Screening* **2014**, *17*, 694−702.
(22) Williams, R. M.; Kulick, A. R.; Yedlapalli, S.; Battistella, L.; Hajiran, C. J.; Sooter, L. J. In vitro selection of a single-stranded DNA molecular recognition element specific for bromacil. *J. Nucleic Acids* **2014**, *2014*, 102968.
(23) Zuker, M. Mfold web server for nucleic acid folding and hybridization prediction. *Nucleic Acids Res.* **2003**, *31*, 3406−3415.
(24) Connell, G. J.; Illangesekare, M.; Yarus, M. Three small ribooligonucleotides with specific arginine sites. *Biochemistry* **1993**, *32*, 5497−5502.
(25) Ellington, A. D.; Khrapov, M.; Shaw, C. A. The scene of a frozen accident. *RNA* **2000**, *6*, 485−498.
(26) Hall, B.; Hesselberth, J. R.; Ellington, A. D. Computational selection of nucleic acid biosensors via a slip structure model. *Biosens. Bioelectron.* **2007**, *22*, 1939−1947.
(27) Lozupone, C.; Changayil, S.; Majerfeld, I.; Yarus, M. Selection of the simplest RNA that binds isoleucine. *RNA* **2003**, *9*, 1315−1322.
(28) Majerfeld, I.; Yarus, M. Isoleucine:RNA sites with associated coding sequences. *RNA* **1998**, *4*, 471−478.
(29) Wiseman, T.; Williston, S.; Brandts, J. F.; Lin, L.-N. Rapid measurement of binding constants and heats of binding using a new titration calorimeter. *Anal. Biochem.* **1989**, *179*, 131−137.
(30) Dutta, A. K.; Rösgen, J.; Rajarathnam, K. Using isothermal titration calorimetry to determine thermodynamic parameters of protein-glycosaminoglycan interactions. *Methods Mol. Biol.* **2015**, *1229*, 315−324.
(31) Zhang, Z.; Oni, O.; Liu, J. New insights into a classic aptamer: binding sites, cooperativity and more sensitive adenosine detection. *Nucleic Acids Res.* **2017**, *45*, 7593−7601.
(32) Alsager, O. A.; Kumar, S.; Willmott, G. R.; McNatty, K. P.; Hodgkiss, J. M. Small molecule detection in solution via the size contraction response of aptamer functionalized nanoparticles. *Biosens. Bioelectron.* **2014**, *57*, 262−268.
(33) Mehta, J.; Rouah-Martin, E.; Van Dorst, B.; Maes, B.; Herrebout, W.; Scippo, M.-L.; Dardenne, F.; Blust, R.; Robbens, J. Selection and characterization of PCB-binding DNA aptamers. *Anal. Chem.* **2012**, *84*, 1669−1676.
(34) Nguyen, V.-T.; Kwon, Y. S.; Kim, J. H.; Gu, M. B. Multiple GO-SELEX for efficient screening of flexible aptamers. *Chem. Commun.* **2014**, *50*, 10513−10516.
(35) McKeague, M.; Velu, R.; Hill, K.; Bardóczy, V.; Mészáros, T.; DeRosa, M. Selection and characterization of a novel DNA aptamer for label-free fluorescence biosensing of ochratoxin A. *Toxins* **2014**, *6*, 2435−2452.
(36) McKeague, M.; De Girolamo, A.; Valenzano, S.; Pascale, M.; Ruscito, A.; Velu, R.; Frost, N. R.; Hill, K.; Smith, M.; McConnell, E. M.; DeRosa, M. C. Comprehensive analytical comparison of strategies used for small molecule aptamer evaluation. *Anal. Chem.* **2015**, *87*, 8608−8612.
(37) Gray, D. M.; Ratliff, R. L.; Vaughan, M. R. [19] Circular dichroism spectroscopy of DNA. *Methods Enzymol.* **1992**, *211*, 389−406.
(38) Kypr, J.; Kejnovska, I.; Renciuk, D.; Vorlickova, M. Circular dichroism and conformational polymorphism of DNA. *Nucleic Acids Res.* **2009**, *37*, 1713−1725.
(39) Patel, D. J.; Suri, A. K.; Jiang, F.; Jiang, L.; Fan, P.; Kumar, R. A.; Nonin, S. Structure, recognition and adaptive binding in RNA aptamer complexes. *J. Mol. Biol.* **1997**, *272*, 645−664.
(40) Lee, B. H.; Nguyen, V. T.; Gu, M. B. Highly sensitive detection of 25-HydroxyvitaminD 3 by using a target-induced displacement of aptamer. *Biosens. Bioelectron.* **2017**, *88*, 174−180.
(41) Wang, P.; Wan, Y.; Ali, A.; Deng, S.; Su, Y.; Fan, C.; Yang, S. Aptamer-wrapped gold nanoparticles for the colorimetric detection of omethoate. *Sci. China: Chem.* **2016**, *59*, 237−242.
(42) Smith, J. E.; Griffin, D. K.; Leny, J. K.; Hagen, J. A.; Chávez, J. L.; Kelley-Loughnane, N. Colorimetric detection with aptamer-gold nanoparticle conjugates coupled to an android-based color analysis application for use in the field. *Talanta* **2014**, *121*, 247−255.
(43) Chávez, J. L.; MacCuspie, R. I.; Stone, M. O.; Kelley-Loughnane, N. Colorimetric detection with aptamer-gold nanoparticle conjugates: effect of aptamer length on response. *J. Nanopart. Res.* **2012**, *14*, 1166.
(44) Ruscito, A.; DeRosa, M. C. Small-Molecule Binding Aptamers: Selection Strategies, Characterization, and Applications. *Front. Chem.* **2016**, *4*, 14.
(45) McKeague, M.; Derosa, M. C. Challenges and opportunities for small molecule aptamer development. *J. Nucleic Acids* **2012**, *2012*, 748913.
(46) Hickey, K. M. *Analytical and Computational Methods for the Assessment of Biological Molecules and Their Binding Interactions: Case Studies in DNA Aptamer-Target Binding and P450-P450 Dimerization Dissertation*; West Virgina University: Morgantown, West Virgina, 2015.

DOI: 10.1021/acsomega.8b01859
ACS Omega 2018, 3, 13576−13583